# Electronic Supplementary Information

Bimetallic Co$_4$Mo$_8$ Cluster Built from Mo$_8$ Oxothiomolybdate Capped by Co$_4$-Thiacalix[4]arene Unit: the Observation of Co-Mo Synergistic Effect for Binder-free Electrocatalyst

Min Zhang,[‡a] Mengwei Chen,[‡a] Yanfeng Bi,[*a] Liangliang Huang,[a] Kun Zhou,[a] and Zhiping Zheng[*b]

[a]College of Chemistry, Chemical Engineering and Environmental Engineering, Liaoning Shihua University, Fushun 113001, P. R. China. biyanfeng@lnpu.edu.cn

[b]Shenzhen Grubbs Institute and Department of Chemistry, Southern University of Science and Technology, Shenzhen, Guangdong 518000, China. E-mail:zhengzp@sustc.edu.cn
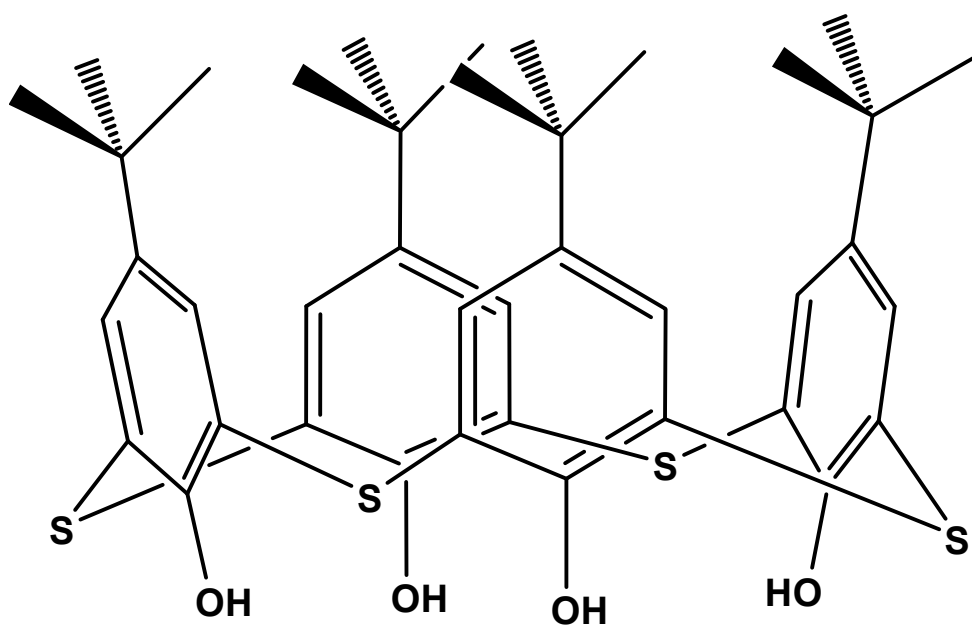
Scheme S1 p-tert-Butylthiacalix[4]arene(H$_4$TC4A)

Note for single crystal X-ray diffraction.

SQUEEZE RESULTS (APPEND TO CIF)
Note: Data are Listed for all Voids in the P1 Unit Cell
i.e. Centre of Gravity, Solvent Accessible Volume,
Recovered number of Electrons in the Void and
Details about the Squeezed Material
loop_
  _platon_squeeze_void_nr
  _platon_squeeze_void_average_x
  _platon_squeeze_void_average_y
  _platon_squeeze_void_average_z
  _platon_squeeze_void_volume
 _platon_squeeze_void_count_electrons
  _platon_squeeze_void_content

1	0.249	0.248	0.504	212	43 ''
2	0.250	0.749	-0.004	212	46 ''
3	0.059	0.649	0.320	9	2 ''
4	0.163	0.254	0.805	18	3 ''
5	0.336	0.754	0.695	18	2 ''
6	0.440	0.149	0.179	9	2 ''
7	0.749	0.251	1.004	212	42 ''
8	0.751	0.751	0.496	212	45 ''
9	0.559	0.851	0.820	9	3 ''
10	0.663	0.246	0.305	18	3 ''
11	0.836	0.746	0.195	18	3 ''
12	0.940	0.351	0.679	9	2 ''

_platon_squeeze_details   ?

SQUEEZE gives four main electron regions per unit cell for **Co_4Mo_8**, which can be assigned to the contributions of four unsolved $CHCl_3$ in the voids. As there are four formula unit per cell, the TENTATIVE formula for the compounds might be:

$\{Co_4(TC4A)Cl[(MoO_2)_2S(CH_3O)]_4\}(NH_4)(CHCl_3)_2$
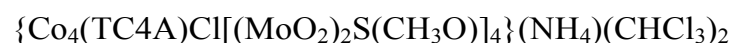
The precession images 0kl (left) and h0l (right) layers of **Co_4Mo_8** are presented below:
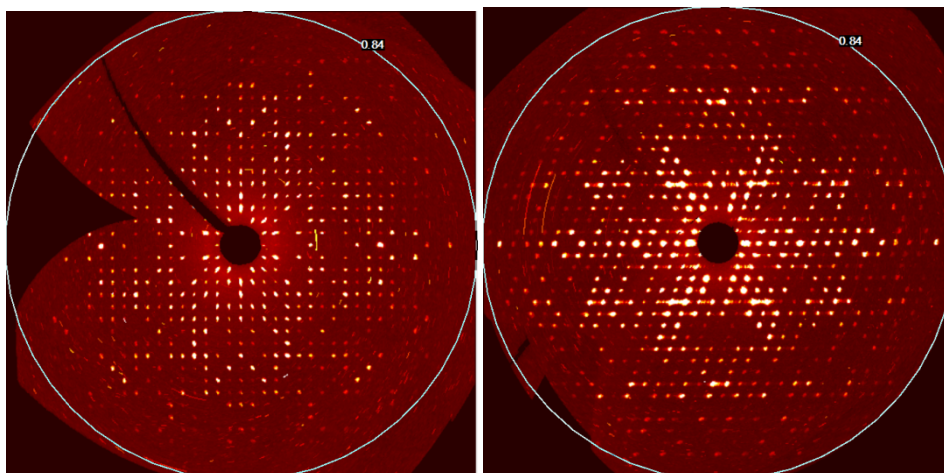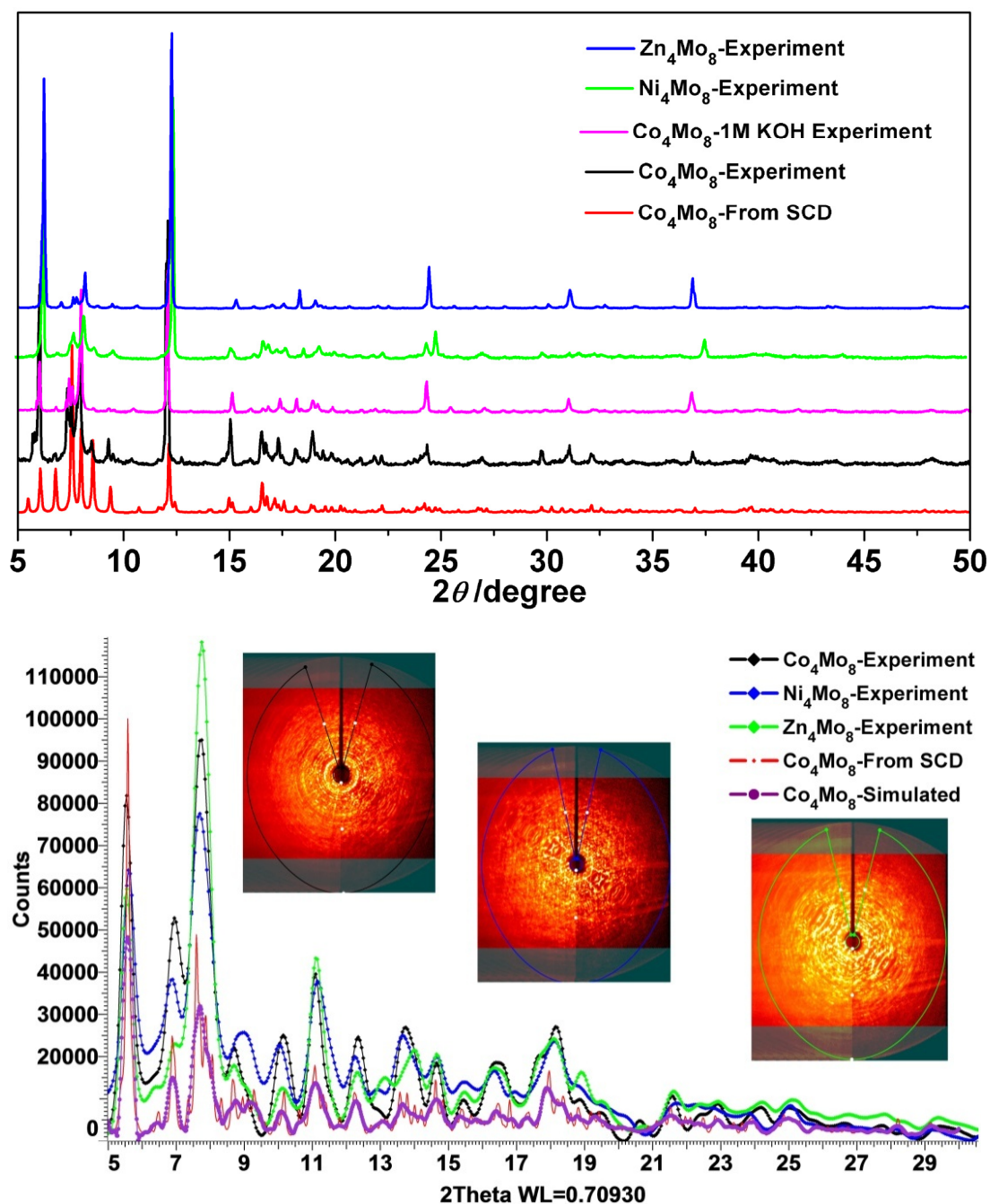
Fig. S1 Power (up) and single-crystal (bottom) X-ray diffraction of Co_4Mo_8, Ni_4Mo_8 and Zn_4Mo_8.

XRD patterns for compound Co_4Mo_8 is accordant with the simulated one derived from the single crystal X-ray data (SCD), confirming the pure phase of the samples of Co_4Mo_8. Power/single-crystal X-ray diffraction confirmed the formation of the isomers of Co_4Mo_8 for Ni_4Mo_8 and Zn_4Mo_8. Furthermore, the XRD of activated Co_4Mo_8 (80 ^{o}C for 10h in vacuum) immersed in 1M KOH for 12 h showed similar peak distributions to Co_4Mo_8 cystals.
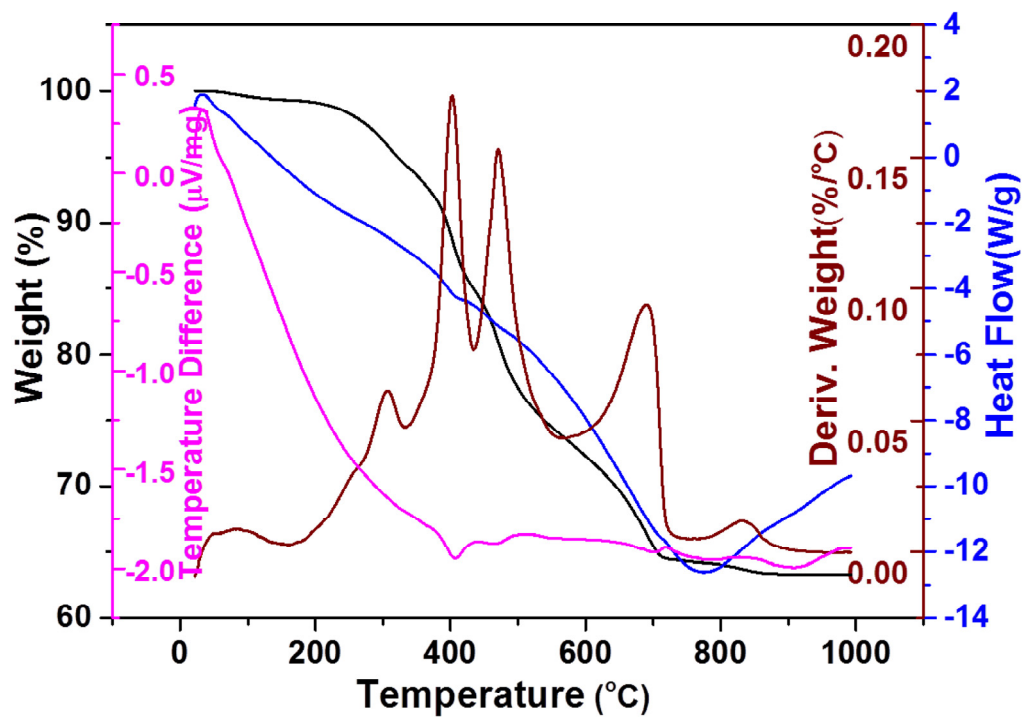
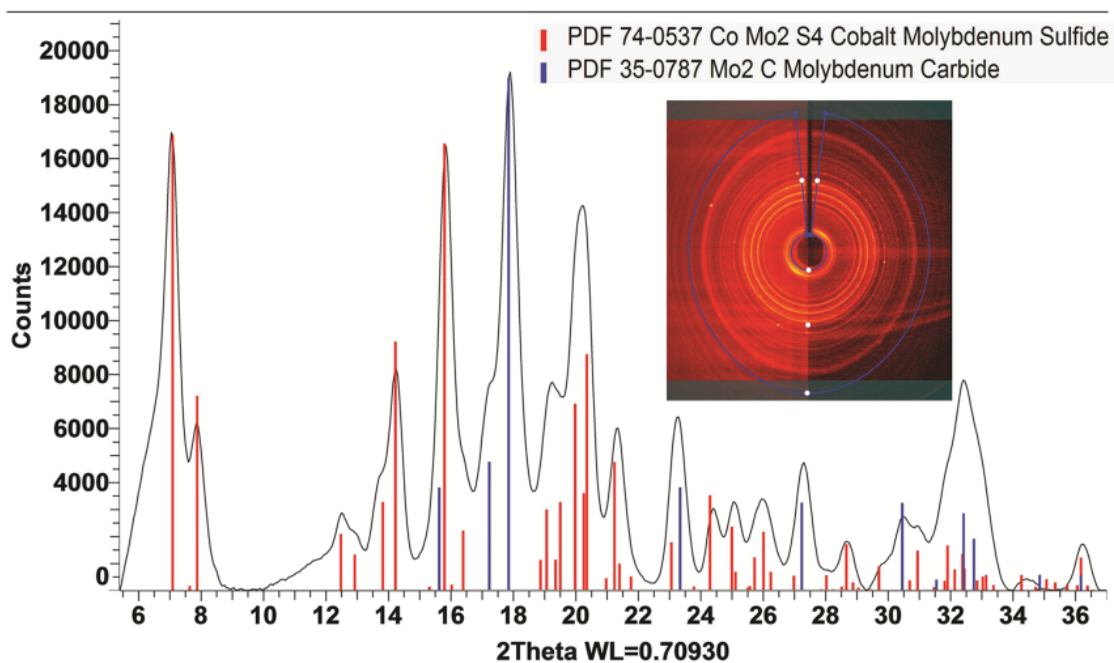**Fig. S2** TGA curves of compound Co_4Mo_8 in N_2.

Fig. S3 The XRD of the final decomposition of TGA. The final decomposition product at 1000°C was found to be the mixture of $CoMo_2S_4$ and Mo_2C.
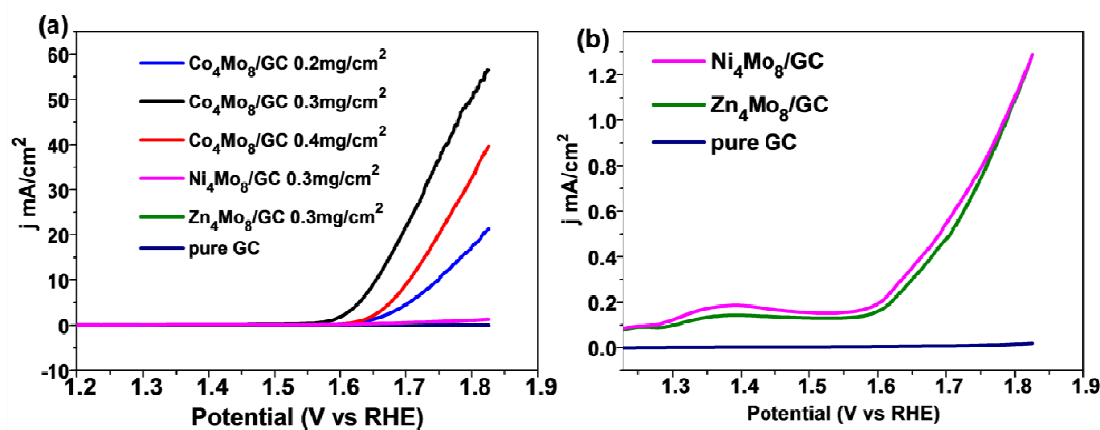
Fig. S4 (a) OER linear sweeping voltammetry (LSV) curves of the **M_4Mo_8** (M = Co, Ni, Zn) materials on GC and pure GC; (b) Amplified LSV of **Ni_4Mo_8**/GC and **Zn_4Mo_8**/GC.
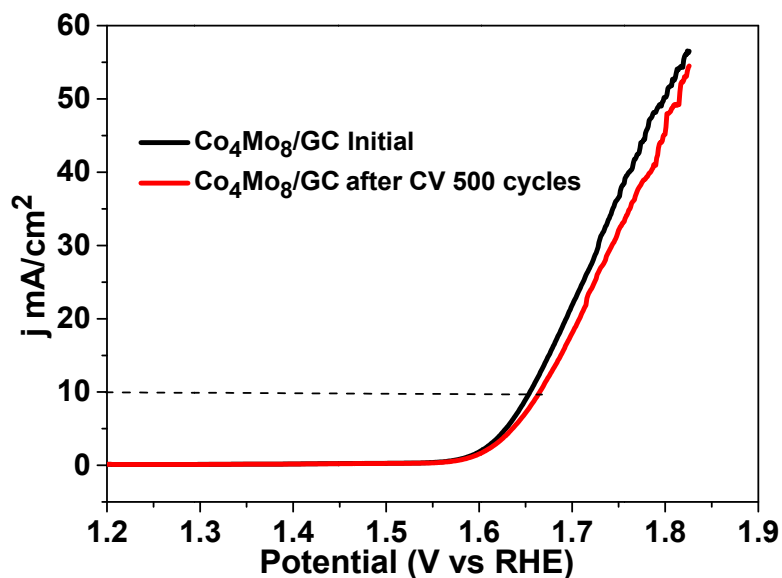
Fig. S5 OER linear sweeping voltammetry curves of the **Co_4Mo_8** (crystal) materials with mass loading 0.3mg/cm^2 on GC.
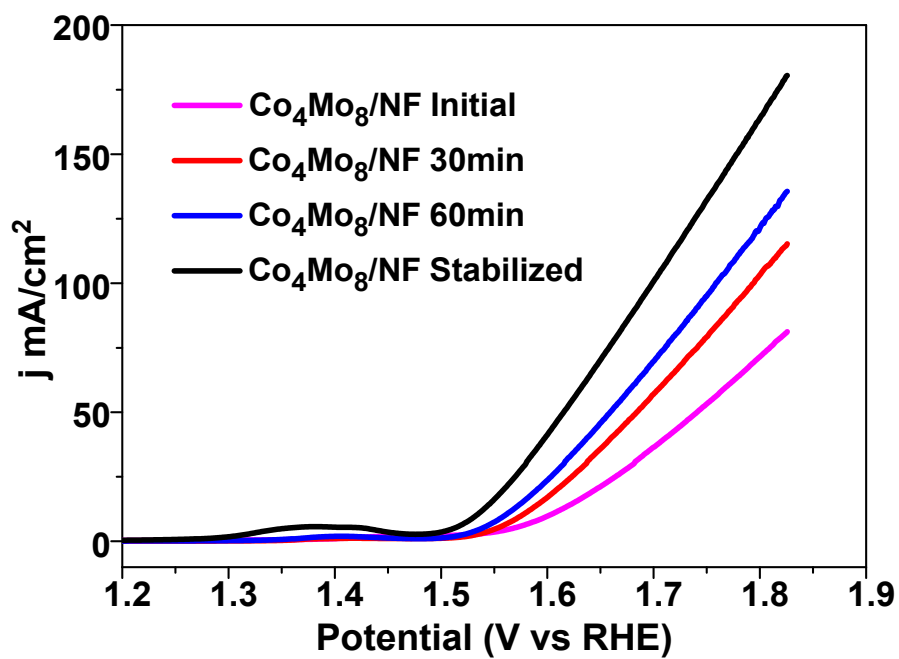
Fig. S6 Time-dependent LSV curves of **Co₄Mo₈**/NF at pH = 14.
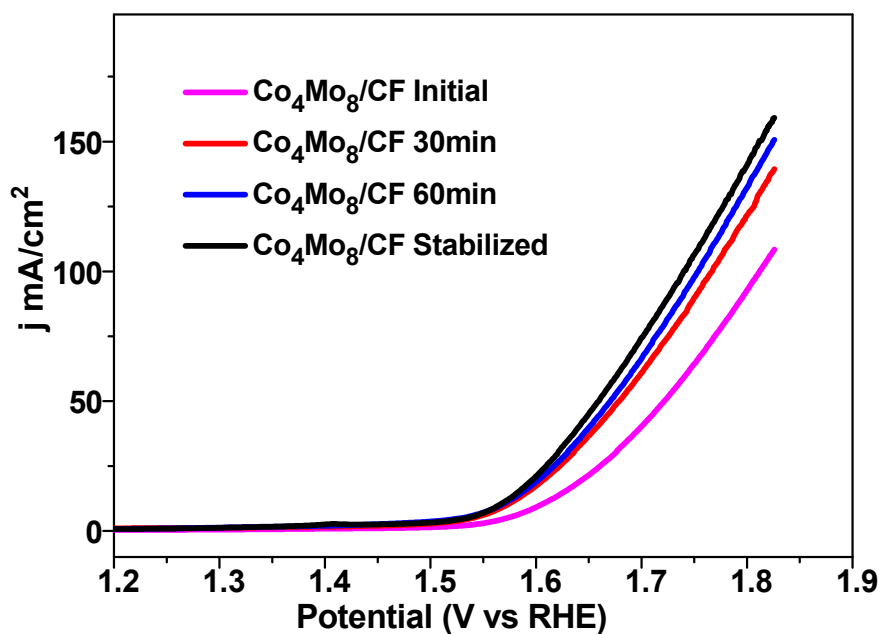
Fig. S7 Time-dependent LSV curves of **Co₄Mo₈**/CF at pH = 14.
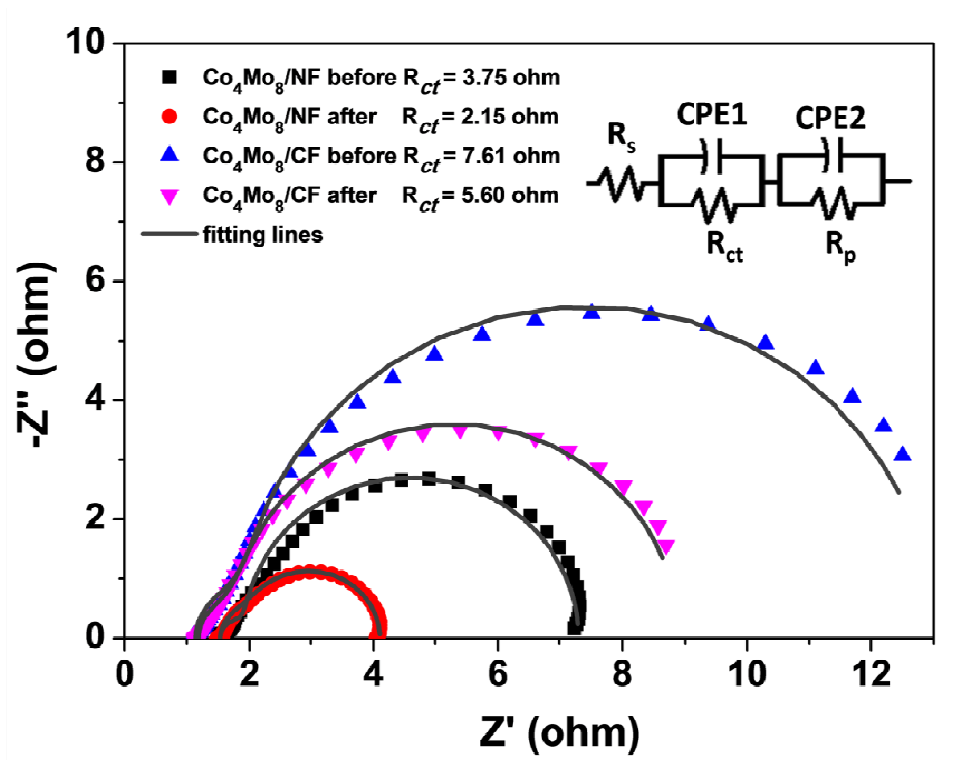
Fig. S8 Nyquist plots of **Co$_4$Mo$_8$**/NF and **Co$_4$Mo$_8$**/CF before and after 24h-long electrocatalytic OER over a frequency range from 0.01 Hz to 10^5 Hz. Insert: the equivalent electric circuit was used to fit the data (Ref. *Angew. Chem. Int. Ed.,* 2018, **57**, 9660).
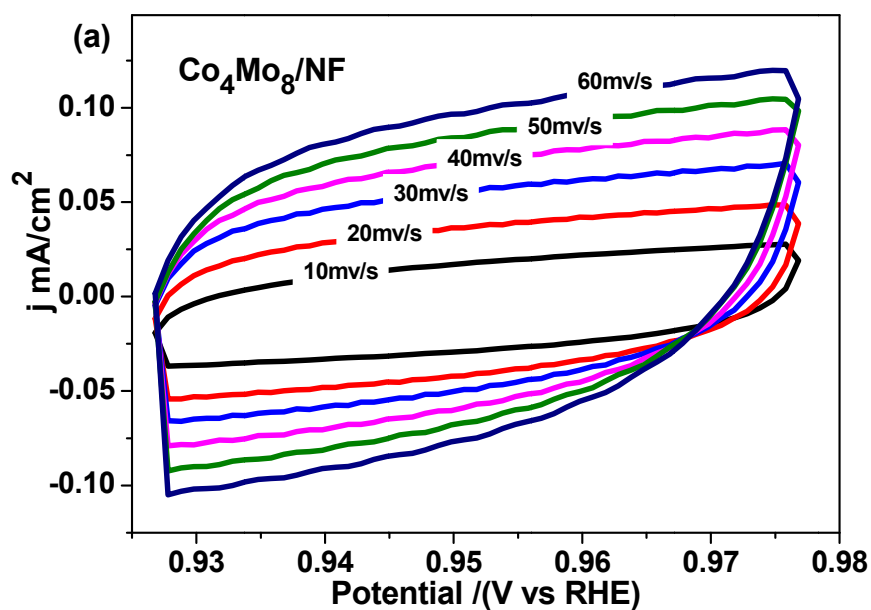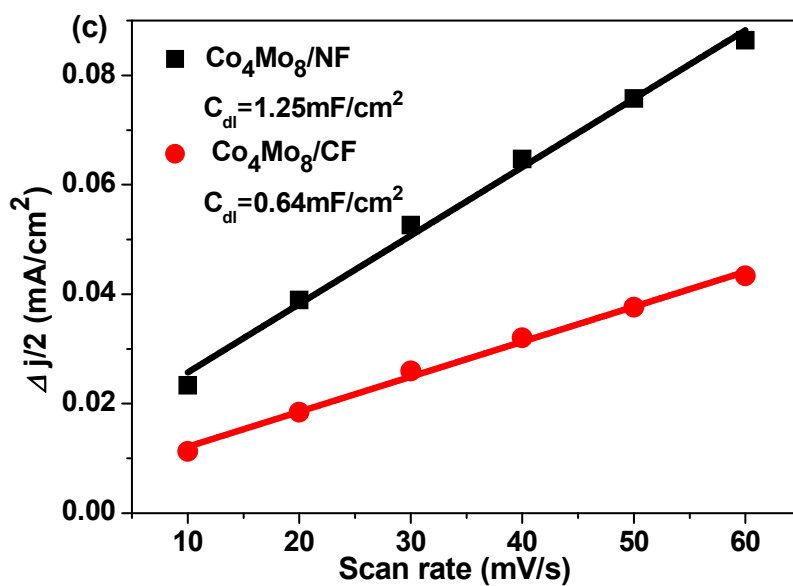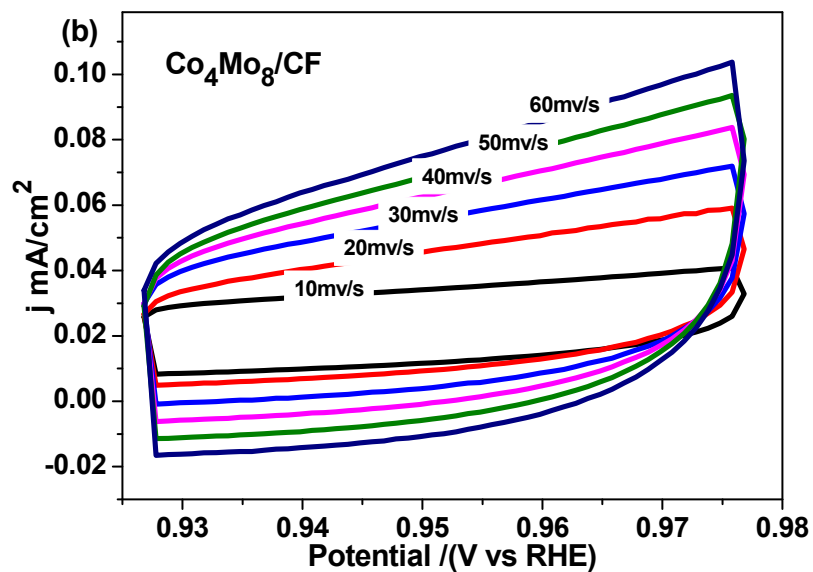
Fig. S9 The cyclic voltammograms (CVs) measurements with various scan rates for (a) **Co₄Mo₈**/NF and (b) **Co₄Mo₈**/CF in 1.0 M KOH; (c) the capacitive current density ($J_a/2-J_c/2$) as a function of scan rate in the region of 0.9268~0.9768 V *vs.* RHE.
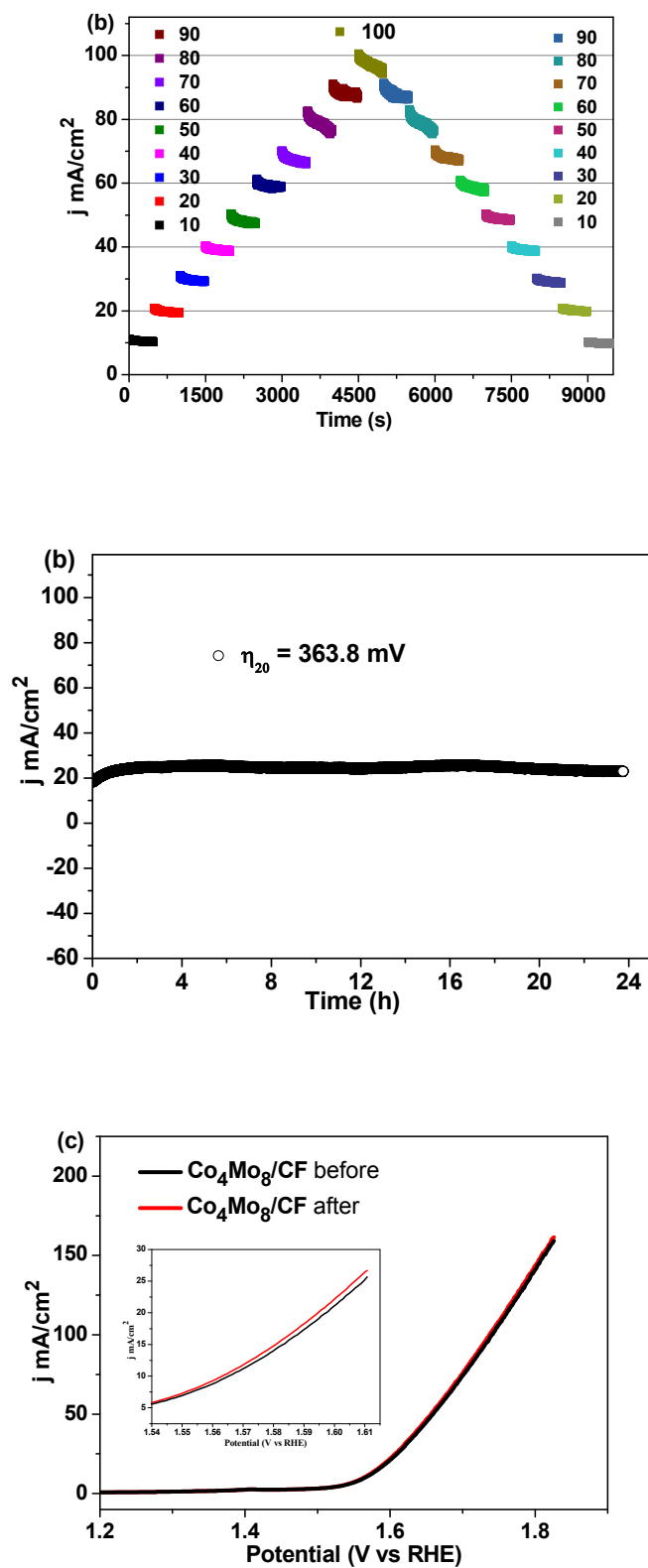
Fig. S10 (a) Stage stability test per 500s for **Co₄Mo₈**/CF; (b) The prolonged chronoamperometric profiles of **Co₄Mo₈**/CF at 363.8 mV for 24h; (c) Polarization curves before and after 24h-long electrocatalytic OER.

(a) Co₄Mo₈/NF initial
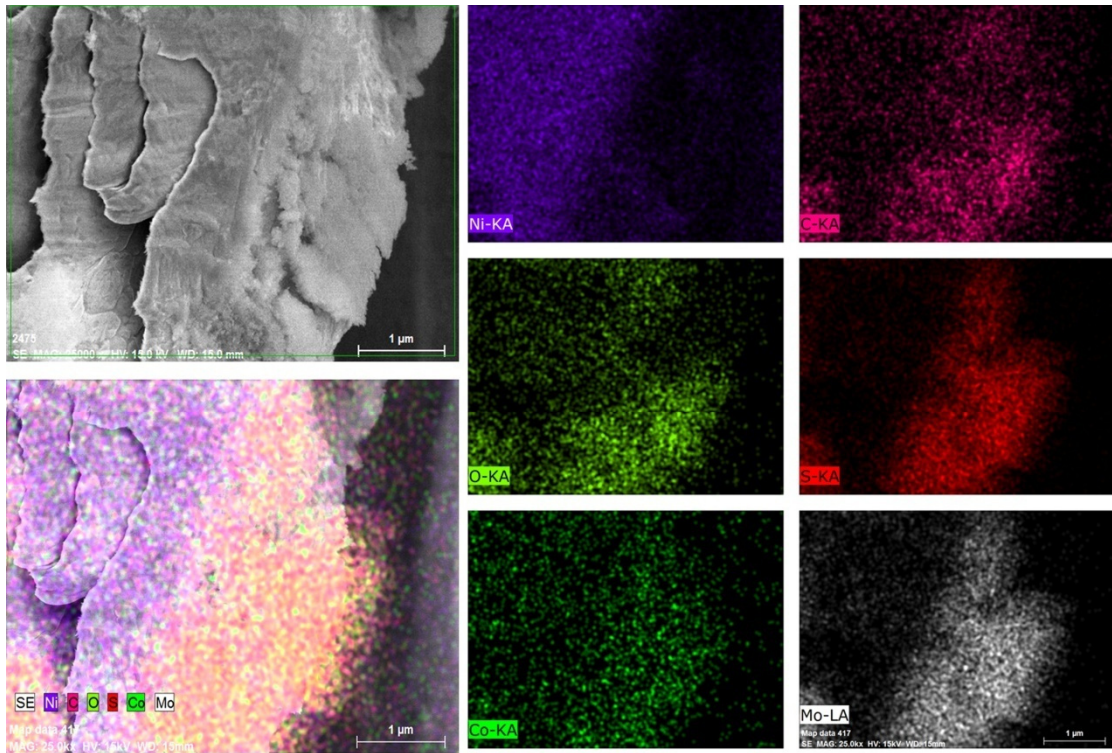
(b) Co₄Mo₈/NF after
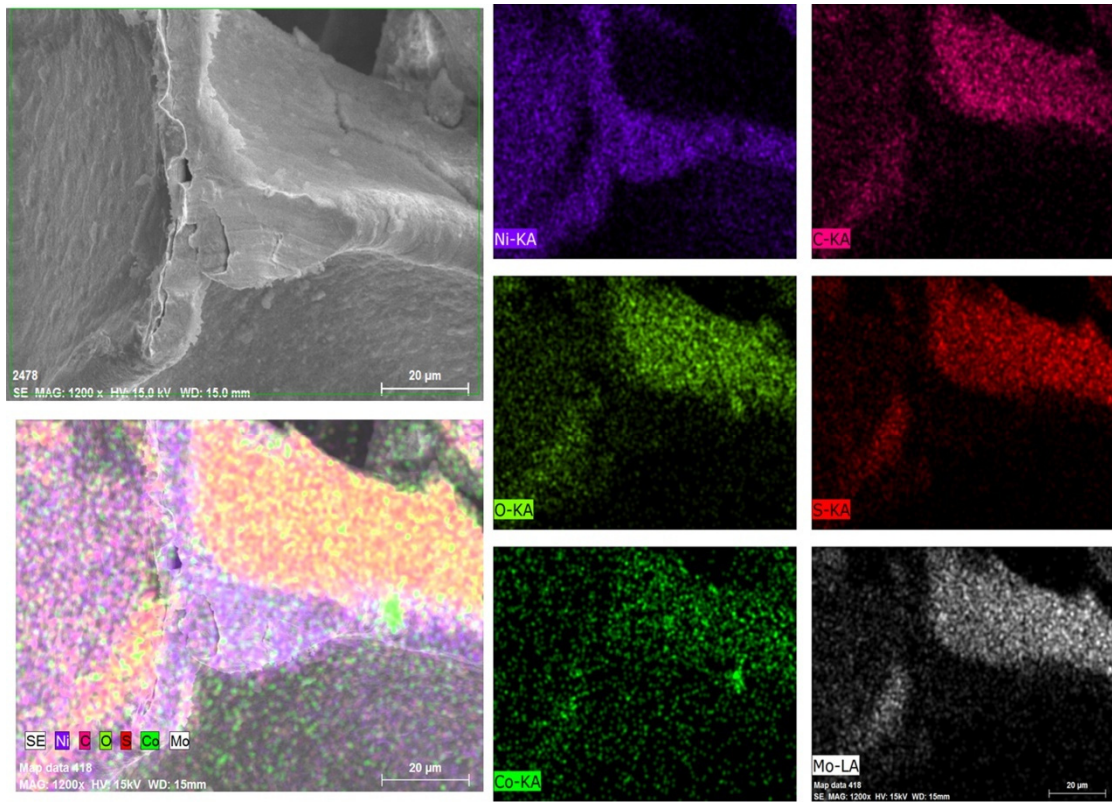
(c) Co$_4$Mo$_8$/CF initial
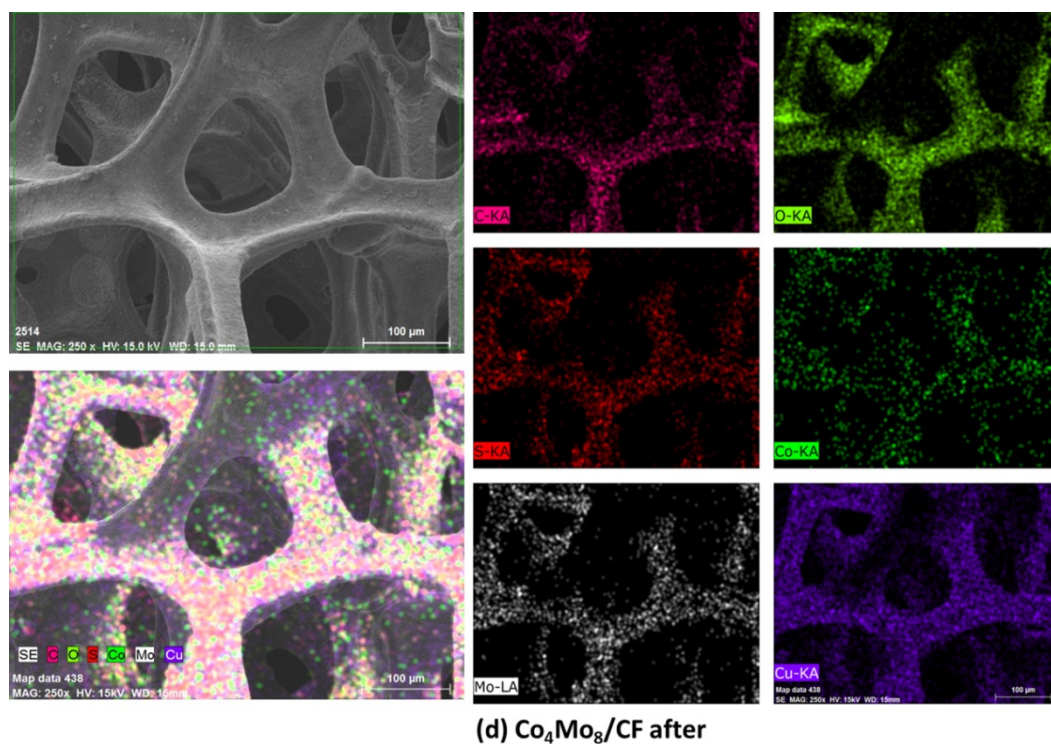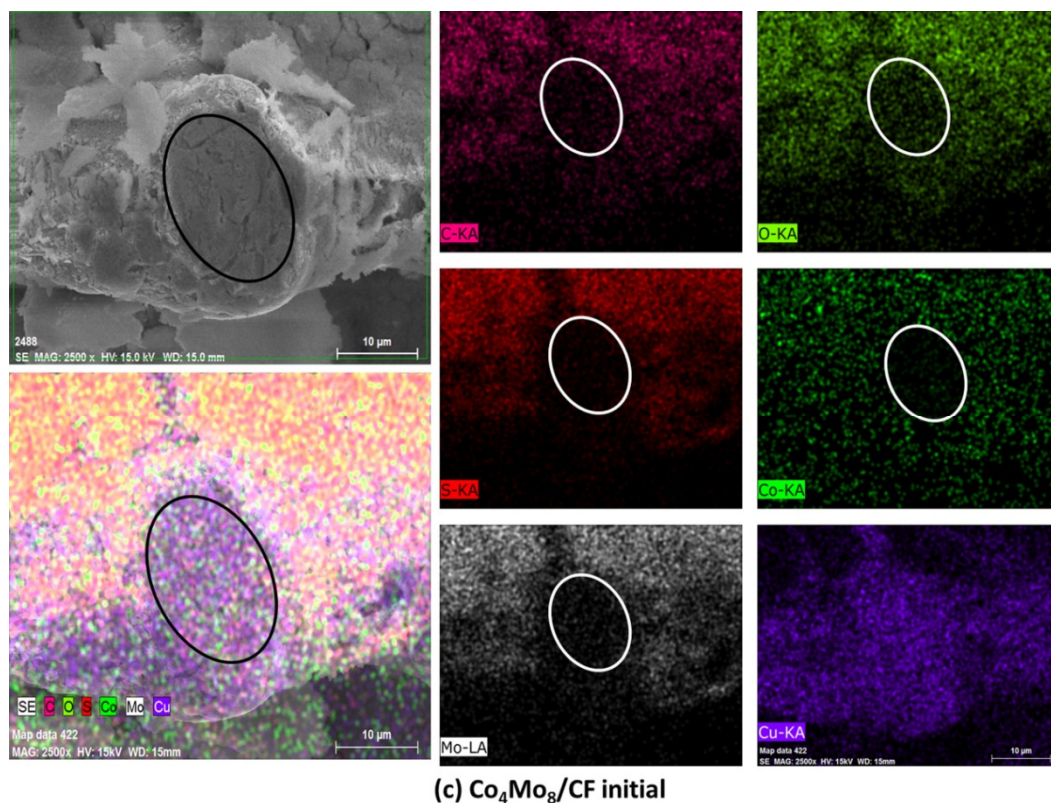
(d) Co$_4$Mo$_8$/CF after

Fig. S11 Scanning electron microscope (SEM) elemental mapping image of {**Co$_4$Mo$_8$**} at different stages: (a) **Co$_4$Mo$_8$**/NF initial, (b) **Co$_4$Mo$_8$**/NF after, (c) **Co$_4$Mo$_8$**/CF initial, and (d) **Co$_4$Mo$_8$**/CF after .

(a) Co₄Mo₈-as synthesized

Element	Atom (%)
Mo	5.45 ± 0.85
Co	3.07 ± 0.42
S	6.06 ± 0.49
Cl	2.00 ± 0.16

(b) Co₄Mo₈- Activated

Element	Atom (%)
Mo	1.42 ± 0.39
Co	0.70 ± 0.13
S	1.71 ± 0.16
Cl	0.30 ± 0.09

Element	Atom (%)
Mo	4.72±0.39
Co	2.59±0.33
S	5.01±0.36
Cl	Not detected
K	0.66±0.06

(c) Co₄Mo₈-as activated-in 1M KOH

Fig. S12 EDX analysis of **Co₄Mo₈** at different stages: (a) **Co₄Mo₈**-as synthesized, (b) **Co₄Mo₈**-Activated and (c) **Co₄Mo₈**-activated-in 1M KOH.
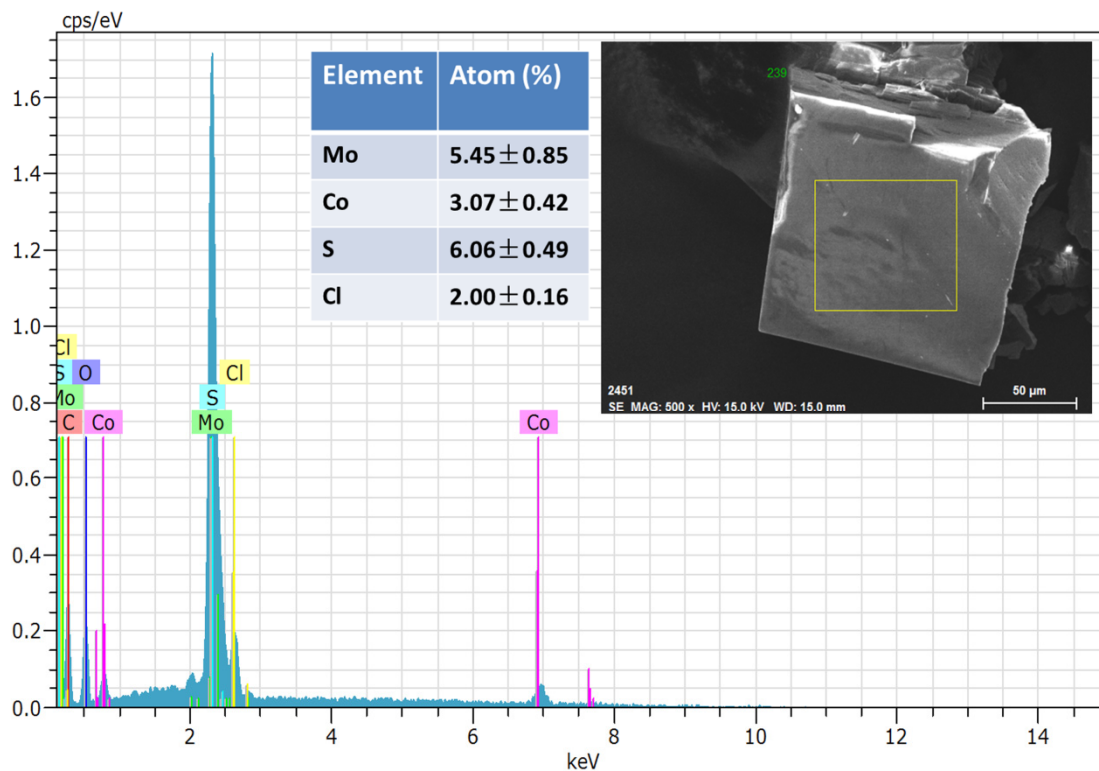
(a) Co₄Mo₈-as synthesized
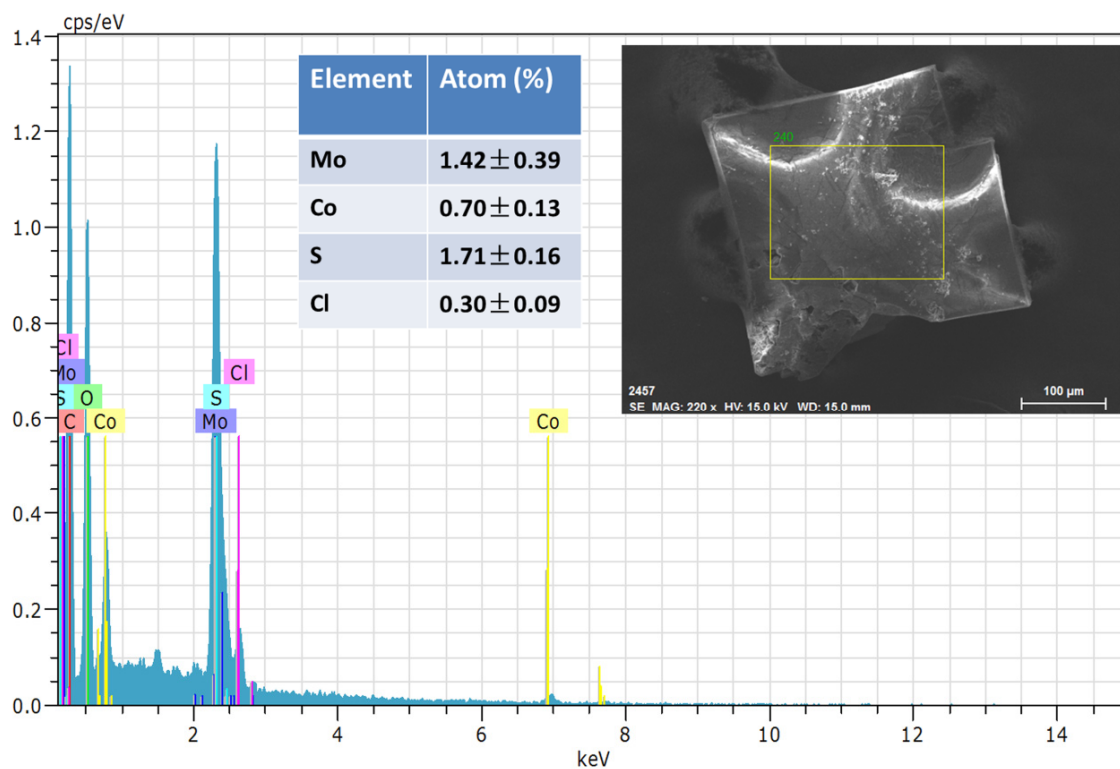
(b) Co₄Mo₈- Activated

(c) Co₄Mo₈-as activated-in 1M KOH
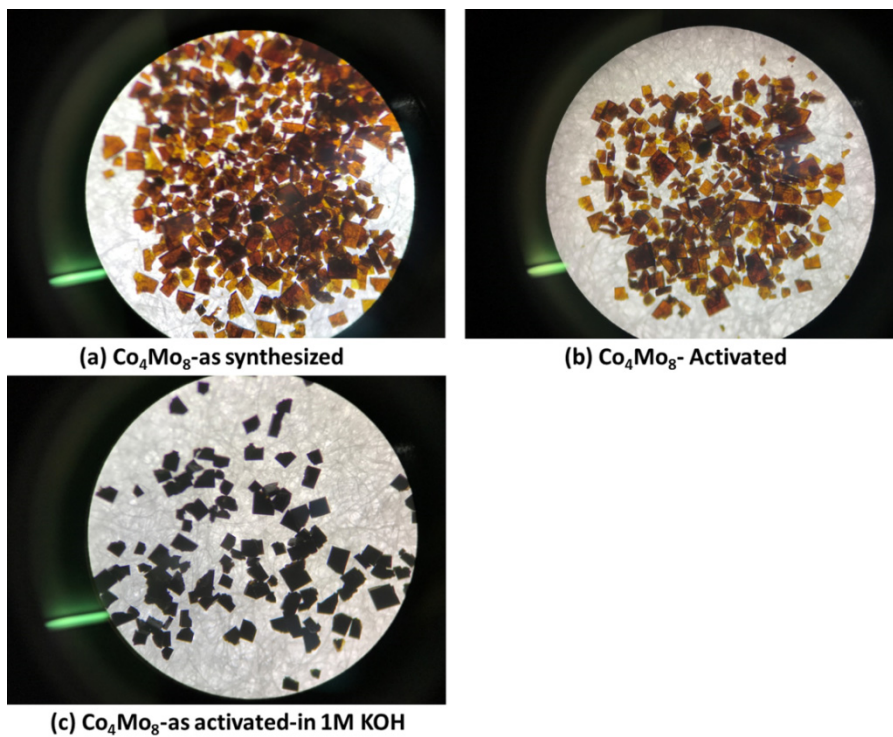
Fig. S13 The microscope of **Co₄Mo₈** at different stages: (a) **Co₄Mo₈**-as synthesized, (b) **Co₄Mo₈**-activated and (c) **Co₄Mo₈**-activated-in 1M KOH.
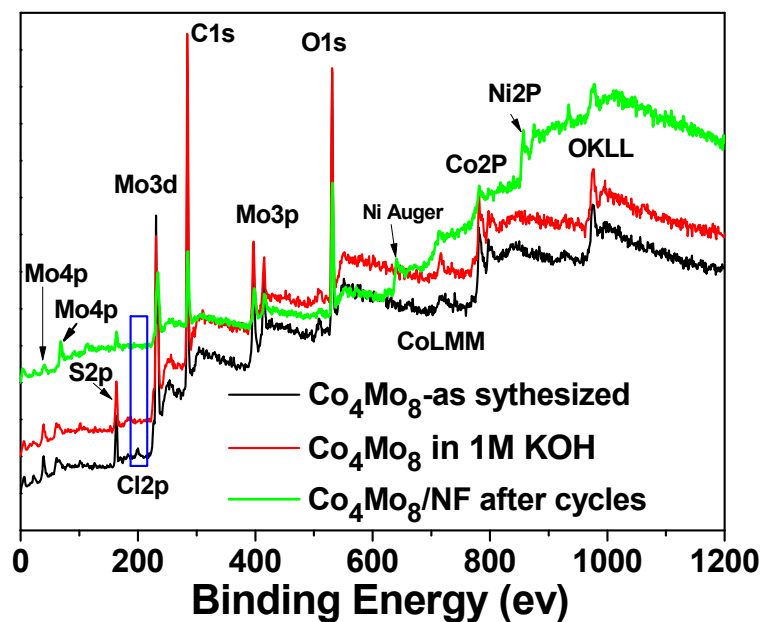
Fig. S14 The XPS survey of **Co₄Mo₈**-as synthesized, **Co₄Mo₈**-activated-in 1M KOH, and **Co₄Mo₈**/NF after cycles (after stabilized LSV).
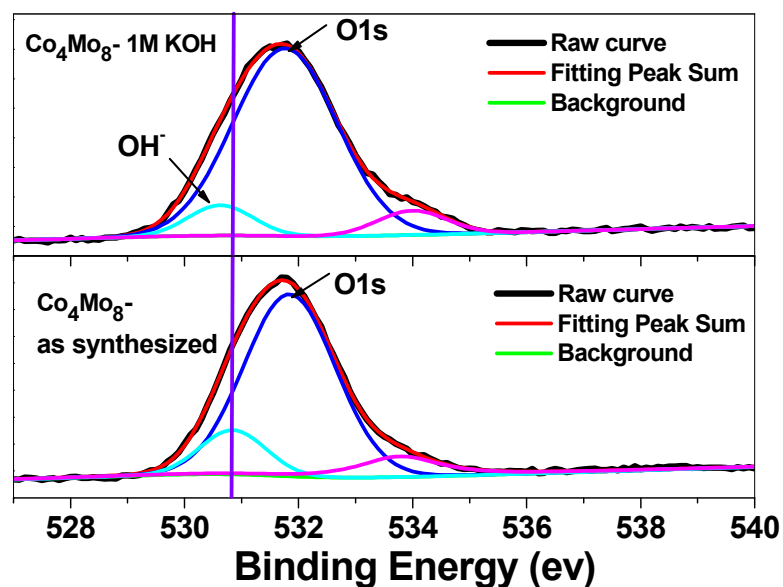
Fig. S15 High-solution O1s XPS of **Co₄Mo₈**-as synthesized and **Co₄Mo₈**-activated-in 1M KOH.
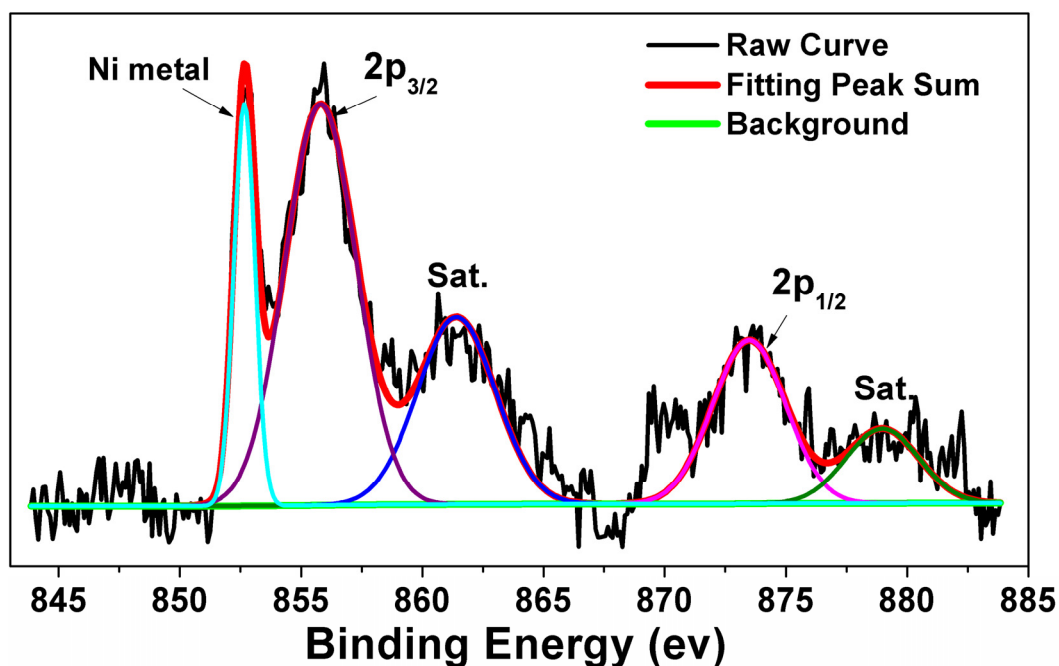
Fig. S16 High-solution Ni2p XPS. The sample was prepared by sonication of **Co₄Mo₈**/NF in methanol/chloroform (1:1) mixture to remove the surface fabricated **Co₄Mo₈**. The obtained XPS shows typical bonding peaks at ca. 852.7 eV that can be assigned to Ni metal. The satellite (Sat.) peak (ca. 861.4 eV) shift to higher binding energy compared with Ni-O analogues (below 861.0 eV) indicated a modified local electronic structure of Ni surface, likely due to the binding between **Co₄Mo₈** and NF, that is, Ni–S signals.

Ref. H.W. Nesbitt, D. Legrand and G.M. Bancroft, Interpretation of Ni2p XPS spectra of Ni conductors and Ni insulators, *Phys. Chem. Minerals.*,2000, **27**, 357-366.
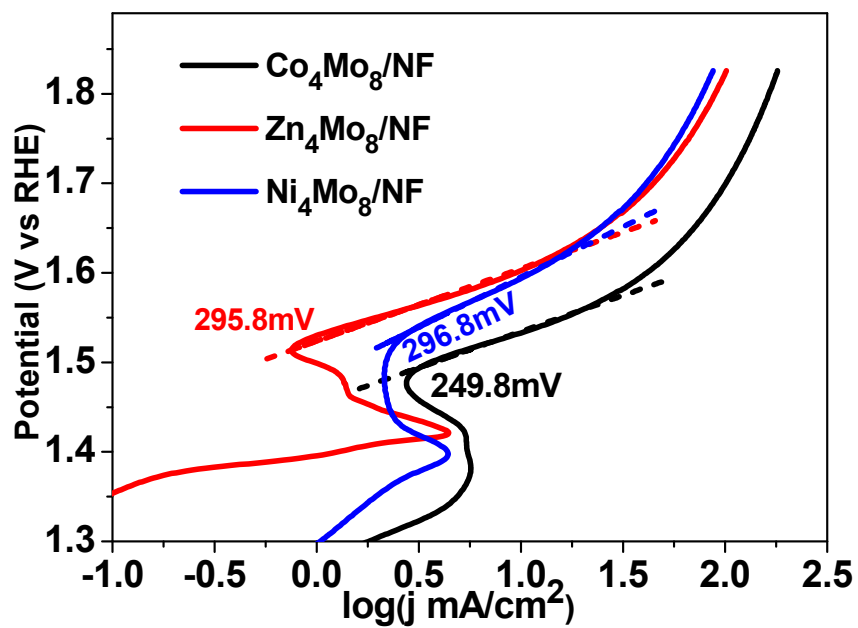
Fig. S17 Comparing onset potential of **Co₄Mo₈**/NF, **Ni₄Mo₈**/NF, and **Zn₄Mo₈**/NF electrodes
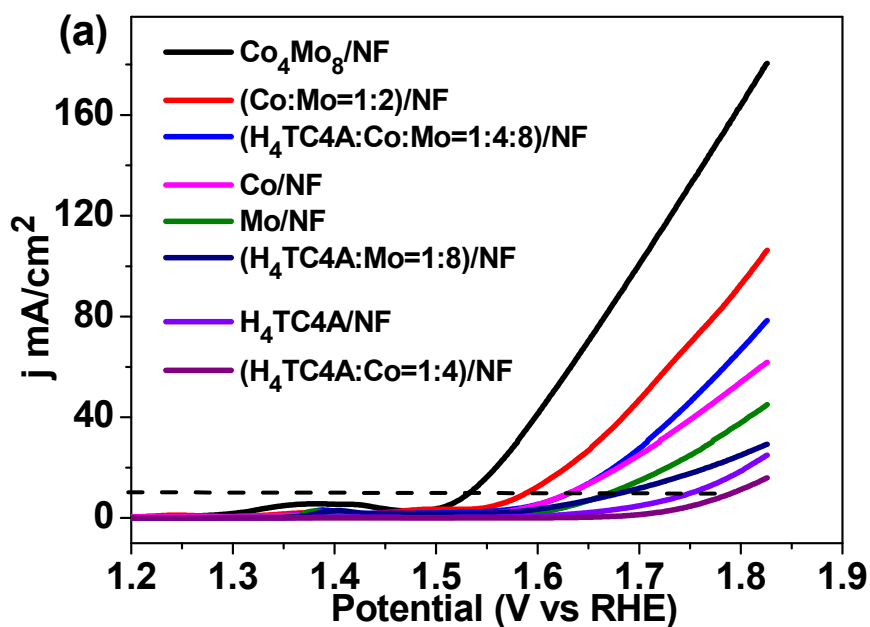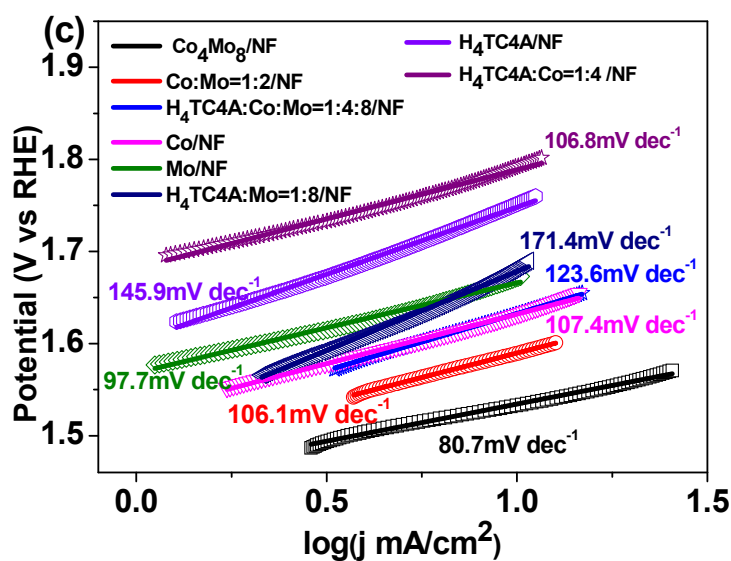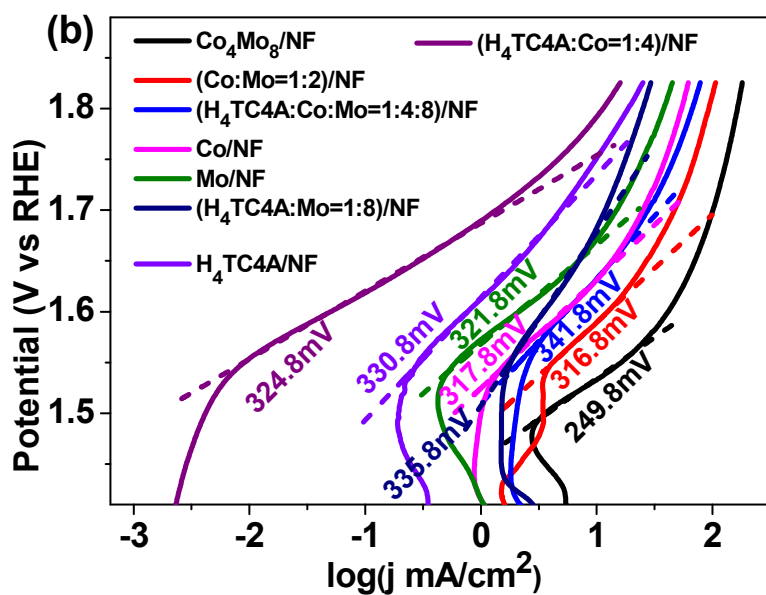
Fig. S18 Single component and simple combination of multiple components polarization curves (LSV) (a), onset potential (b) and tafel plots (c) of (Co:Mo=1:2)/NF, (H₄TC4A:Co:Mo=1:4:8)/NF, Co/NF, Mo/NF, (H₄TC4A:Mo=1:8)/NF, H₄TC4A/NF, (H₄TC4A:Co=1:4)/NF (Co: Co(CH₃COO)₂·4H₂O; Mo: (NH₄)₂MoS₂O₂) in 1 M KOH solution at a scan rate of 5 mV/s.
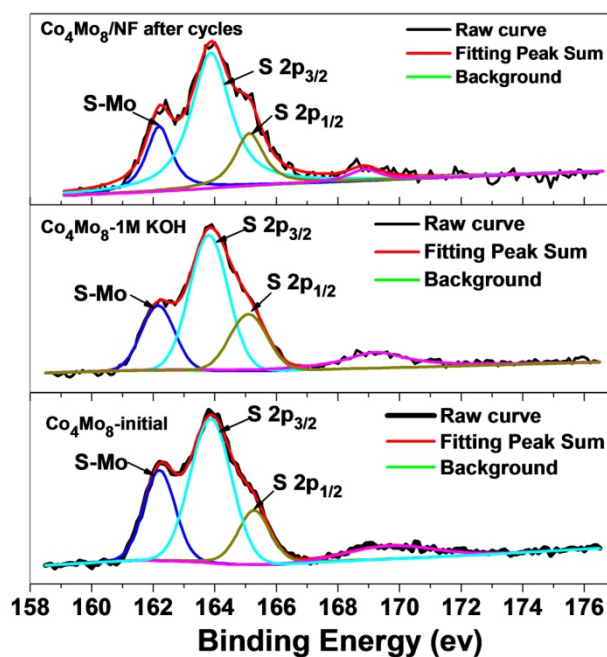
Fig. S19 High-solution S2p XPS of **Co₄Mo₈**-as synthesized and **Co₄Mo₈**-activated-in 1M KOH.

Table S1 Crystal data and structural refinement parameters for $(NH_4)_2MoS_2O_2$ and **Co₄Mo₈**

Formula	$H_8MoN_2O_2S_2$	$C_{45}H_{61}Cl_4Co_4Mo_8NO_{24}S_8$
Mr	228.16	2397.52
Crystal system	Monoclinic	Monoclinic
space group	$C2/c$ (No. 15)	$P2_1/n$ (No. 14)
Temperature (K)	296	296
a(Å)	11.4090(14)	16.9518(9)
b(Å)	7.3036(6)	17.0056(9)
c(Å)	9.4236(18)	30.0349(14)
$α$(°)	90	90
$β$(°)	117.389(3)	104.113(2)
$γ$(°)	90	90
Volume($Å^3$)	697.22(17)	8397.0 (7)
Z	4	4
D_c(g/cm³)	2.174	1.896
$μ$(mm⁻¹)	2.394	2.304
Reflections collected	3472	100895
Unique data(R_{int})	611	14879
GOF on F^2	1.05	1.06
R_1 [I>2sigma(I)]	0.0175	0.0896
wR_2	0.0438	0.2593

$^aR_1 = Σ||F_0|-|F_c||/Σ|F_0|$; $^bwR_2 = \{Σ[w(F_0^2-F_c^2)^2]/Σ[w(F_0^2)^2]\}^{1/2}$

Table S2 Selected bond distances (Å) and BVS calculations for **Co₄Mo₈**

Band	Distance	r	Value	Band	Distance	r	Value
Co(1)-O(4)	1.934(10)	1.692	0.520	Mo(3)-O(15)	1.692(12)	1.907	1.788
Co(1)-O(1)	1.978(5)	1.692	0.462	Mo(3)-O(7)	1.964(10)	1.907	0.857
Co(1)-O(5)	2.051(9)	1.692	0.379	Mo(3)-O(6)	1.991(11)	1.907	0.797
Co(1)-O(12)	2.083(10)	1.692	0.348	Mo(3)-O(21)	2.056(11)	1.907	0.669
Co(1)-S(1)	2.499(4)	2.06	0.305	Mo(3)-S(6)	2.300(5)	2.35	1.145
Co(1)-Cl(1)	2.687(4)	2.01	0.160	valence			5.256
valence			2.174	Mo(4)-O(16)	1.682(13)	1.907	1.837
Co(2)-O(3)	1.952(10)	1.692	0.495	Mo(4)-O(7)	1.952(10)	1.907	0.885
Co(2)-O(4)	1.991(10)	1.692	0.446	Mo(4)-O(8)	1.984(10)	1.907	0.812
Co(2)-O(11)	2.073(9)	1.692	0.357	Mo(4)-O(22)	2.081(10)	1.907	0.625
Co(2)-O(10)	2.075(10)	1.692	0.355	Mo(4)-S(6)	2.315(5)	2.35	1.099
Co(2)-S(4)	2.500(4)	2.06	0.304	valence			5.258
Co(2)-Cl(1)	2.685(4)	2.01	0.161	Mo(5)-O(17)	1.681(11)	1.907	1.842
valence			2.118	Mo(5)-O(9)	1.948(10)	1.907	0.895
Co(3)-O(2)	1.954(10)	1.692	0.493	Mo(5)-O(8)	2.000(10)	1.907	0.778
Co(3)-O(3)	1.983(10)	1.692	0.455	Mo(5)-O(22)	2.081(11)	1.907	0.625
Co(3)-O(9)	2.054(10)	1.692	0.376	Mo(5)-S(7)	2.302(5)	2.35	1.139
Co(3)-O(8)	2.083(10)	1.692	0.348	valence			5.279
Co(3)-S(3)	2.511(4)	2.06	0.296	Mo(6)-O(18)	1.672(12)	1.907	1.887
Co(3)-Cl(1)	2.680(4)	2.01	0.164	Mo(6)-O(9)	1.941(10)	1.907	0.912
valence			2.132	Mo(6)-O(10)	1.995(10)	1.907	0.788
Co(4)-O(1)	1.952(10)	1.692	0.495	Mo(6)-O(23)	2.097(10)	1.907	0.598
Co(4)-O(2)	1.992(10)	1.692	0.444	Mo(6)-S(7)	2.324(5)	1.907	1.073
Co(4)-O(7)	2.045(10)	1.692	0.385	valence			5.258
Co(4)-O(6)	2.079(10)	1.692	0.351	Mo(7)-O(19)	1.671(11)	1.907	1.892
Co(4)-S(2)	2.505(4)	2.06	0.300	Mo(7)-O(11)	1.958(10)	1.907	0.871
Co(4)-Cl(1)	2.676(4)	2.01	0.165	Mo(7)-O(10)	2.003(10)	1.907	0.771
valence			2.140	Mo(7)-O(23)	2.089(10)	1.907	0.611
Mo(1)-O(13)	1.675(12)	1.907	1.872	Mo(7)-S(8)	2.295(5)	2.35	1.160
Mo(1)-O(5)	1.957(10)	1.907	0.874	valence			5.305
Mo(1)-O(12)	2.002(10)	1.907	0.774	Mo(8)-O(20)	1.664(12)	1.907	1.929
Mo(1)-O(24)	2.084(10)	1.907	0.620	Mo(8)-O(11)	1.941(9)	1.907	0.912
Mo(1)-S(5)	2.307(5)	2.35	1.123	Mo(8)-O(12)	1.984(10)	1.907	0.812
valence			5.263	Mo(8)-O(24)	2.094(10)	1.907	0.603
Mo(2)-O(14)	1.655(13)	1.907	1.976	Mo(8)-S(8)	2.314(5)	2.35	1.102
Mo(2)-O(5)	1.953(9)	1.907	0.883	valence			5.358
Mo(2)-O(6)	1.989(10)	1.907	0.801				
Mo(2)-O(21)	2.098(11)	1.907	0.597				
Mo(2)-S(5)	2.315(5)	2.35	1.099				
valence			5.356				

Table. S3 Potential and Tafel slope of the reported electrocatalysts for OER. (η: overpotential)

Catalyst	onset potential (mV)	η_{10} (mV)	Tafel (mV/ dec)
Co_4Mo_8/NF	249.8	302.8	80.7
Co_4Mo_8/CF	269.8	332.8	109.1
Co_4Mo_8/GC	326.8	423.8	112.6
Pure NF	-	562.8	-
Pure CF	-	592.8	-
Zn_4Mo_8/NF	295.8	371.8	81.0
Ni_4Mo_8/NF	296.8	362.8	112.2
(Co:Mo=1:2)/NF	316.8	358.8	106.1
(H_4TC4A:Co:Mo=1:4:8)/NF	341.8	401.8	123.6
Co/NF	317.8	400.8	107.4
Mo/NF	321.8	440.8	97.7
(H_4TC4A:Mo=1:8)/NF	335.8	451.8	171.4
H_4TC4A/NF	330.8	520.8	145.9
(H_4TC4A:Co=1:4)/NF	324.8	561.8	106.8

Table. S4 Comparison of the OER performances of recently reported active catalysts with that in this work. **Precious-metal oxides, Co-based Bimetal MOFs, Co-based MOFs, Catalystsform MOF precursors** and **related Co-based Bimetal composite materials** are grouped and highlighted with different background colors.

Catalyst	Electrolyte	overpotential (mV) (at 10mA/cm^2)	Substrate/Binder	Tafel Slope (mV/dec)	Mass loading (mg/cm^2)	TOF (s^{-1})	Reference
Co$_4$Mo$_8$	1.0 M KOH	302.8	NF/none	80.67	0.8± 0.1	0.52-0.67×10^{-2}(300mV)	**This work**
Zn$_4$Mo$_8$		371.8	NF/none	112.16	0.8± 0.1	0.057-0.074×10^{-2} (300mV)	
Ni$_4$Mo$_8$		362.8		81.04	0.8± 0.1	0.16-0.20×10^{-2} (300mV)	
Co$_4$Mo$_8$		332.8	CF/none	109.14	0.8± 0.1	0.27-0.35×10^{-2} (300mV)	
		423.8	GC//Nafion	112.6	0.3	0.055×10^{-2} (300mV)	
IrO$_2$/C (20 wt%)	0.1 M KOH	370	GCE/Nafion	-	0.2	4.4×10^{-2}(300mV)	S1. *Nat. Commun.,* 2013, **4**, 2390.
RuO$_2$	1.0 M KOH	330	GCE/Nafion	-	0.2	0.47×10^{-2} (300mV)	S2. *J. Mater. Chem. A,* 2015, **3**, 17763.
Fe/Ni$_{2.4}$/Co$_{0.4}$-MIL-53	1.0 M KOH	219	GCE/Nafion	53.5	0.51	-	S3. *Angew. Chem. Int. Ed.,* 2018, **130,**1888.
Fe/Ni$_{2.4}$/Co$_{0.4}$-MIL-53		238 @100mA/cm^2	NF/none	71.3	-	-	
Bulk NiCo-MOFs	1.0 M KOH	317	GCE/Nafion	61	0.2	0.15 (300mV)	S4. *Nat. Energy,* 2016, **1**, 16184.
NiCo-UMOFNs		250	GCE/Nafion	42	0.2	0.86 (300mV)	
FeTPyP-Co	0.1 M NaOH	351@1 mA/cm^2	Au/null	-	-	12.2 (310mV)	S5. *J. Am. Chem. Soc.,* 2016, **138**, 3623.

Material	Electrolyte	Overpotential	Electrode/Binder	Tafel slope	Mass loading	TOF (potential)	Reference
CoFe-MOFs-1.7	1.0 M KOH	319	RDE/Nafion	56	0.424	$0.42/0.66\times10^{-2}$ for Co/Fe (280mV)	S6. *ACS Appl. Mater. Inter,* 2017,**9**, 362.
Fe$_3$-Co$_2$	0.1 M KOH	225	NF/Nafion	48	0.22	0.61-1.82 (300mV)	S7. *J. Am. Chem. Soc.,* 2017, **139**, 1778.
		237	CF/Nafion	79	0.22	0.24-0.71 (300mV)	
		283	GCE/Nafion	43	0.22	0.27 (300mV)	
Co:Fe$_3$		453	GCE/Nafion	63	0.22	$0.031\text{-}0.088\times10^{-2}$ (300mV)	
NNU-21(Fe$_3$-BPTC)	0.1 M KOH	555	Carbon cloth/Nafion	122.7	1.0	0.1×10^{-2} (400mV)	S8. *Angew. Chem. Int. Ed.,* 2018, **57**,9660.
NNU-22(Fe$_2$Co-BPTC)		376		77.2		1.8×10^{-2} (400mV)	
NNU-23(Fe$_2$Ni-BPTC)		365		81.8		2.0×10^{-2} (400mV)	
NNU-24(Fe$_2$Zn-BPTC)		522		121.8		0.2×10^{-2} (400mV)	
Co-ZIF-9	pH =13.4	510@1 mA/cm^2	FTO glass/Nafion	93	0.2	0.058×10^{-2} (300mV)	S9. *Nanoscale.,* 2014, **6**, 9930.
Co(C1$_2$H$_6$O$_4$)(H$_2$O)$_4$]	0.1 M KOH	520	Cu Foil/none	142	~0.2	0.013×10^{-2} (300mV)	S10. *J. Am. Chem. Soc.,* 2014, **136**, 13925.
Co-WOC-1	0.1 M KOH	390@1 mA/cm^2	GCE/Nafion	128	0.283	1.1×10^{-2} (400mV)	S11. *Angew. Chem. Int. Ed.,* 2016, **55**, 2425.
Co-MOF	1.0 M KOH	311@50 mA/cm^2	NF/none	77	5.84	0.18 (400mV)	S12. *Inorg. Chem. Front.,* 2018, **5**, 344.

Catalyst	MOF precursor		Overpotential	Substrate	Tafel			Reference
Co-MOF Powder			362@50 mA/cm²	NF/none	89	-		
Co-TBSC		1.0 M KOH	290	NF/Nafion	75	-	-	S13. *J. Mater. Chem. A.,* 2017, **5**, 23559.
MAF-X27-OH		1.0 M KOH	387	GCE/Nafion	60	0.18	$0.14 \times 10^{-2}/3.8 \times 10^{-2}$ (300/400mV)	S14. *J. Am. Chem. Soc.,*2016, **138**, 8336.
			338	Cu Foil/none	82	0.23	$0.74 \times 10^{-2}/9.6 \times 10^{-2}$ (300/400mV)	
Co-UTSA-16		1.0 M KOH	370	GCE/Nafion	77	~0.35	-	S15. *ACS Appl. Mater. Interfaces.,* 2017, **9**, 7193
Catalyst	MOF precursor							
$CoFe_2O_4$/C NRAs	MOF-74–Co/Fe	1.0 M KOH	240	NF@NC	45	1.03	0.53×10^{-2} (300mV)	S16. *Adv. Mater.,* 2017, **29**, 1604437.
$CoFe_2O_4$/C powders			310		61	1.03	0.33×10^{-2} (300mV)	
NiCoP/C	ZIF-67@LDH	1.0 M KOH	330	GCE	96	-	-	S17. *Angew. Chem. Int. Ed.,* 2017, **56**, 3897
NiCoP			370	GCE	115			
Ni-Co LDH nanoboxes			420	GCE	135			
Co_3S_4@MoS_2	ZIF-67	1.0 M KOH	330	GCE	88	0.283	-	S18. *Chem. Mater.,* 2017, **29**, 5566.
Ni@CoO@CoNC	Ni@CoO@ZIF-67	1.0 M KOH	309	NF	53	4.0	-	S19. *Chem.,* 2017, **2**, 791.
$NiCo_2O_4$‖$Ni_{0.33}Co_{0.67}S_2$ nanowires		1.0 M KOH	420@5 mA/cm²	Ti foil/none	60	0.3	-	S20. *Adv. Energy Mater.,* 2015, **5**, 1412031.
CoMn LDH		1.0 M KOH	324	GCE/Nafion	43	0.142	7.5×10^{-2} (300mV)	S21. *J. Am. Chem. Soc.,* 2014, **136**, 16481.
$ZnCo_2O_4$		1.0 M KOH	390	Pt-Ti alloy coated glass	46	-	-	S22. *J. Phys. Chem. Lett.,* 2014, **5**, 2370.
CoCo LDH		1.0 M KOH	393	GCE/Nafion	59	0.07	-	S23. *Nat. Commun.,* 2014, **5**, 4477.

NiCo LDH	1.0 M KOH	367	Carbon paper	40	0.17	-	S24. *Nano let.*, 2015, **15**, 1421.
CoNi nanosheets	1.0 M KOH	450	GCE/Nafion	56.8	-	-	S25. *Chem. Sci.*, 2015, **6**, 3572.
CoFe nanosheets		380		44.9			
CoNi/C		360		38.5			
CoFe/C		300		61			
$Ni_xCo_{3-x}O_4$ nanowire array	1.0 M KOH	~370	Ti foil	120	~3.0	-	S26. *Adv. Mater.*, 2010, **22**, 1926.
Ni-Co-mixedoxide nanocages	1.0M KOH	380	GCE/Nafion	50	-	-	S27. *Adv. Mater.*, 2016, **28**, 4601.
Ni-substituted Co_3O_4 Nanowire array	1.0 M NaOH	~370	NF	65-75	-	-	S28. *Int. J. Hydrogen Energy*, 2011, **36**,72.
$Co_{0.5}Fe_{0.5}S@N-MC$	1.0 M KOH	410	GCE/Nafion	159	0.8	-	S29. *ACS Applied Materials & Interfaces*, 2015, **7**, 1207.
$Mn_3O_4/CoSe_2$	0.1 M KOH	450	GCE/Nafion	49	0.2	-	S30. *J. Am. Chem. Soc.*, 2012, **134**, 2930
$NiCo_{2.7}(OH)_x$	1.0 M KOH	350	GCE/Nafion	65	-	0.18 (350mV)	S31. *Adv. Energy Mater.*, 2015, **5**, 1401880.
CoMnP	1.0 M KOH	330	GCE/Nafion	61	0.284	-	S32. *J. Am. Chem. Soc.*, 2016, **138**, 4006.
$Fe-mCo_3O_4$	1.0 M KOH	380	GCE/Nafion	60	-	2.6×10^{-2} (400mV)	S33. *Chem. Commun.*, 2014, **50**, 10122.
$NiCo_2O_4$ nanowires	1.0 M KOH	460	FTO	90	1.0	1.23×10^{-2} (600mV)	S34. *J. Mater. Chem. A*, 2014, **2**, 20823.
$NiCo_2O_4$ nanoneedles	1.0 M KOH	565	FTO	292	0.53	-	S35. *J. Phys. Chem. C*, 2014, **118**, 25939.
Ni-Co oxide (10 at% Co)	1.0 M NaOH	325	nanoporous layer	39	-	-	S36. *ACS nano*, 2014,**8**, 9518.
Hollow Ni-Co oxide nanosponges	0.1 M KOH	362	GCE/Nafion	64.4	0.2	-	S37. *Chem. Commun.*, 2015, **51**, 7851.

NiCo$_2$O$_4$	0.1 M KOH	390	GCE/Nafion	87	-	-	S38. *Nanoscale*, 2014, **6**, 3173.
Co$_3$O$_4$@CoO SC		430	GCE/Nafion	89		4.87×10^{-2} (400mV)	
IrO$_2$	PH=13.6	411	GCE/Nafion	91	0.025	21.52×10^{-2} (400mV)	S39. *Nat. Commun.*, 2015, **6**, 8106.
RuO$_2$		358	GCE/Nafion	55		53.09×10^{-2} (400mV)	
Co$_3$O$_4$-CuCo$_2$O$_4$	0.1M KOH	498	GCE/Nafion	-	~0.12	-	S40. *Chem. Mater.*, 2013, **25**, 4926.
NiCo LDH	1.0 M KOH	367	Carbonpaper	40	~0.17	-	S41. *Nano Lett.*, 2015, **15**, 1421.
porous N-doped grapheneNiCo$_2$O$_4$	0.1 M KOH	434	hybrid films	156	-	-	S42. *Acs Nano.*, 2013, **7**, 10190.
NiCo$_2$S$_4$@N/S-doped graphene	0.1 M KOH	470	GCE/Nafion	-	~0.283	-	S43. *ACS Appl. Mater. Interfaces,* 2013, **5**, 5002.
Co/Mo$_2$C/Co$_6$Mo$_6$C$_2$/NCRGO		430	GCE/Nafion	45			
Co$_6$Mo$_6$C$_2$/NCRGO	1.0 M KOH	260	GCE/Nafion	50	~0.14	-	S44. *ACS Appl. Mater. Interfaces,* 2017, **9**, 16977.
Co$_6$Mo$_6$C$_2$/Co$_6$Mo$_6$C/NCRGO		400	GCE/Nafion	58			
Co-Mo-C/NRGO-1		330	GCE/Nafion	42			
IrO$_2$	1.0 M KOH	387	GCE/Nafion	77	~0.14	-	S45. *J. Mater. Chem. A*, 2016, 4, 18100.
Mo$_2$C/Co$_6$Mo$_6$C$_2$/NRGO		360	GCE/Nafion	50			
P-Mn$_x$Co$_{3-x}$O$_{4-\delta}$	0.1 M KOH	350	RRDE/Nafion	85	-	0.25	S46. *Chem.-Eur.J.*, 2014, **20**, 12669.
Co-Mo-S	1.0 M KOH	300	Carbon cloth	78	1	-	S47. *Nanoscale*, 2018, **10**, 8404.

Note: NF: nickel foam; CF: copper foam; GCE: glassy carbon electrode, for GCE, the catalysts were coated with Nafion binder; RDE: rotating disk electrode; FTO: fluorine-doped tin oxide; LDH: Layered double hydroxides; H$_2$TPyP: 5,10,15,20-tetra(4-pyridyl)-*21H,23H*-porphyrine; TBSC: *p-tert*-butylsulfonylcalix[4]arene;

NF@NC: Nitrogen doped carbon coated on nickel foam; Co-WOC-1: H_3BTB = 1,3,5-benzenetribenzoic acid; dpe =1,2-di(4-pyridyl)ethylene; RRDE = Rotating ring-disk electrode.

Turnover frequency (TOF) of the catalysts: Based on the LSV, TOF = $(j \times A)/(4 \times F \times m)$, where j is the current density (mA/cm^2) at a given overpotential, A is the surface area of the nickel foam (NF, 1 cm^2), F is the faraday constant (96485 C/mol), m is the moles of active sites on the electrode, respectively. All the catalytically related metal atoms were assumed to be accessible for catalysis the OER.

Supporting Information References:

S1   Y. Zhao, R. Nakamura, K. Kamiya, S. Nakanishi and K. Hashimoto, *Nat. Commun.*, 2013, **4**, 2390-2396.

S2   T. T. Gao, Z. Y. Jin, M. Liao, J. L. Xiao, H. Y. Yuan and D. Xiao, *J. Mater. Chem. A.*, 2015, **3**,17763-17770.

S3   F. L. Li, Q. Shao, X. Q. Huang and J. P. Lang, *Angew. Chem. Int. Ed.*, 2018, **130**, 1888-1892.

S4   S. L. Zhao, Y. Wang, J. C. Dong, C. T. He, H. J. Yin, P. F. An, K. Zhao, X. F. Zhang, C. Gao, L. J. Zhang, J. W. Lv, J. X. Wang, J. Q. Zhang, A. M. Khattak, N. A. Khan, Z. X. Wei, J. Zhang, S. Q. Liu, H. J. Zhao and Z. Y. Tang, *Nat. Energy.* 2016, **1**, 16184-16193.

S5   B. Wurster, D. Grumelli, D. Hötger, R. Gutzler and K. Kern, *J. Am. Chem. Soc.,* 2016, **138**, 3623-3626.

S6   T. Zhang, J. Du, P. X. Xi and C. L. Xu, *ACS Appl. Mater. Interfaces.,* 2016, **9**, 362-370.

S7   J. Q. Shen, P. Q. Liao, D. D. Zhou, C. T. He, J. X. Wu, W. X. Zhang, J. P. Zhang and X. M. Chen, *J. Am. Chem. Soc.,* 2017, **139**, 1778-1781.

S8   X. L. Wang, L. Z. Dong, M. Qiao, Y. J. Tang, J.Liu, Y. F. Li, S. L. Li, J. X. Su and Y. Q. Lan, *Angew. Chem. Int. Ed.,* 2018, **57**, 9660-9664.

S9   S. B. Wang, Y. D. Hou, S. Lin and X. C. Wang, *Nanoscale,* 2014, **6**, 9930-9934.

S10 T. Y. Ma, S. Dai, M. Jaroniec and S. Z. Qiao, *J. Am. Chem. Soc.,* 2014, **136**, 13925-13931.

S11 P. Manna, J. Debgupta, S. Bose and S. K. Das, *Angew. Chem. Int. Ed.*, 2016, **55**, 2425-2430.

S12 X. P. Zhang, W. D. Sun, H. T. Du, R. M. Kong and F. L. Qu, *Inorg. Chem. Front.,* 2018, **5**, 344-347.

S13 N. Bhuvaneswari, K. P. Annamalai, F. R. Dai and Z. N. Chen, *J. Mater. Chem. A.*, 2017, **5**, 23559–23565.

S14 X. F. Lu, P. Q. Liao, J. W. Wang, J. X. Wu, X. W. Chen, C. T. He, J. P. Zhang, G. R. Li and X. M. Chen,*J. Am. Chem. Soc.,* 2016, **138**, 8336-8339.

S15 J. Jiang, L. Huang, X. M. Liu and L. H. Ai,*ACS Appl. Mater. Interfaces.,* 2017, **9**, 7193−7201.

S16 X. F. Lu, L. F. Gu, J. W. Wang, J. X. Wu, P. Q. Liao and G. R. Li, *Adv. Mater.,* 2017, **29**, 1604437-1604443.

S17 P. L. He, X. Y. Yu and X. W. (D.) Lou, *Angew. Chem. Int. Ed.,*2017, **56**, 3897-3900.

S18 Y. N. Guo, J. Tang, H. Y. Qian, Z. L. Wang and Y. Yanmauchi. *Chem. Mater.,*2017, **29**, 5566-5573.

S19 G. R. Cai, W. Zhang, L. Jiao, S. H. Yu and H. L. Jiang, *Chem.,* 2017, **2**, 791-802.

S20 Z. Peng, D. S. Jia, A. M. Al-Enizi, A. A. Elzatahry and G. F. Zheng, *Adv. Energy Mater.,* 2015, **5**, 1402031-1402037.

S21 F. Song and X. Hu, *J. Am. Chem. Soc.,* 2014, **136**, 16481-16484.

S22 T. W. Kim, M. A Woo, M. Regis and K. S. Choi, *J. Phys. Chem. Lett.,* 2014, **5**, 2370-2374.

S23 F. Song and X. Hu, *Nat. Commun.,* 2014, **5**, 4477-4485.

S24 H. F., Liang, F. Meng, M. Cabán-Acevedo, L. S. Li, A. Forticaux, L. C. Xiu, Z. C. Wang and S. Jin, *Nano let.,* 2015, **15**, 1421-1427.

S25 B. Ni and X. Wang, *Chem. Sci.,* 2015, **6**, 3572-3576.

S26 B. Y. G. Li, P. Hasin and Y. Y. Wu, *Adv. Mater.,* 2010, **22**, 1926-1929.

S27 L. Han, X. Y. Yu and X. W. (D.) Lou, *Adv. Mater*., 2016, **28**, 4601-4605.

S28 B. G. Lu, D. X. Cao, P. Wang, G. L. Wang and Y. Y. Gao, *Int. J. Hydrogen Energy.,* 2011, **36**, 72-78.

S29 M. X. Shen, C. P. Ruan, Y. Chen, C. H. Jiang, K. L. Ai and L. H. Lu, *ACS Appl. Mater. Interfaces,* 2015, **7**, 1207-1218.

S30 M. R. Gao, Y. F. Xu, J. Jiang, Zheng Y. R. and S. H. Yu, *J. Am. Chem. Soc.,* 2012, **134**, 2930-2933.

S31 J. W. Nai, H. J. Yin, T. T. You, L. R. Zheng, J. Zhang, P. X. Wang, Z. Jin, Y. Tian, J. Z. Liu, Z. Y. Tang and L. Guo, *Adv. Energy Mater.,* 2015, **5**, 1401880-1401886.

S32 D. Li, H. Baydoun, C. N. Verani and S. L. Brock, *J. Am. Chem. Soc.,* 2016, **138**, 4006-4009.

S33 C. L. Xiao, X. Y. Lu and C. Zhao, *Chem. Commun.,* 2014, **50**, 10122-10125.

S34 X. X. Yu, Z. J. Sun, Z. P. Yan, B. Xiang, X. Liu and P. W. Du, *J. Mater. Chem. A.,* 2014, **2**, 20823-20831.

S35 H. J. Shi and G. H. Zhao, *J. Phys. Chem. C.*, 2014, **118**, 25939-25946.

S36 Y. Yang, H. L. Fei, G. D. Ruan, C. S. Xiang and J. M. Tour, *ACS nano.*, 2014, **8**, 9518-9523.

S37 C. Z. Zhu, D. Wen, S. Leubner, M. Oschatz, W. Liu, M. Holzschuh, F. Simon, S. Kaskel and A. Eychmüller, *Chem. Commun.,* 2015, **51**, 7851-7854.

S38 M. Prabu, K. Ketpang and S. Shanmugam, *Nanoscale.,* 2014, **6**, 3173-3181.

S39 C. W. Tung, Y. Y. Hsu, Y. P. Shen, Y. X. Zheng, T. S. Chan, H. S. Shen, Y. C. Cheng and H. M. Chen, *Nat. Commun.,* 2015, **6**, 8106-8115.

S40 T. Grewe, X. H. Deng, C. Weidenthaler, F. Schüth and H. Tüysüz, *Chem. Mater.,* 2013, **25**, 4926-4935.

S41 H. F. Liang, F. Meng, M. Cabán-Acevedo, L. S. Li, A. Forticaux, L. C. Xiu, Z. C. Wang and S. Jin, *Nano Lett.*, 2015, **15**, 1421-1427.

S42 S. Chen and S. Z. Qiao, *Acs Nano.,* 2013, **7**, 10190-10196.

S43 Q. Liu, J. T. Jin and J. Y. Zhang, *ACS Appl. Mater. Interfaces.*, 2013, **5**, 5002-5008.

S44 Y. J. Tang, C. H. Liu, W. Huang, X. L. Wang, L. Z. Dong, S. L. Li and Y. Q. Lan, *ACS Appl. Mater. Interfaces.,* 2017, **9**, 16977-16985.

S45 C. H. Liu, Y. J. Tang, X. L. Wang, W. Huang, S. L. Li, L. Z. Dong and Y. Q. Lan, *J. Mater. Chem. A.,* 2016, **4**, 18100-18106.

S46 T. Y. Ma, S. Dai, M. Jaroniec and S. Z. Qiao, *Chem.-Eur. J.,* 2014, **20**, 12669-12676.

S47 Y. J. Tang, A. M. Zhang, H. J. Zhu, L. Z. Dong, X. L. Wang, S. L. Li, M. Han, X. X. Xu and Y. Q. Lan, *Nanoscale.,* 2018, **10**, 8404-8412.